JOURNAL OF GUIDANCE, CONTROL, AND DYNAMICS
Vol. 20, No. 5, September–October 1997

New Results for an Asymmetric Rigid Body with Constant Body-Fixed Torques

Rafael Livneh* and Bong Wie†
Arizona State University, Tempe, Arizona 85287

The rotational motion of an asymmetric rigid body under the influence of constant body-fixed torque is investigated. A set of nondimensional equations of motion is introduced for the stability analysis of equilibrium points. In particular, three-dimensional phase space trajectories are developed for two different cases: 1) constant torque along the major or minor axis and 2) constant torque along the intermediate axis. For both cases, some new analytical as well as simulation results are presented in terms of equilibrium manifolds, separatrix surfaces, periodic or nonperiodic solutions, and extrema of the periodic solutions.

Introduction

TOGETHER with Newton's second law, Euler's rotational equations of motion derived in 1758 are among the cornerstones of classical mechanics. As discussed by Leimanis,[1] the simplest problem for an asymmetric rigid body next to the torque-free case is that of self-excitation whereby the asymmetric rigid body is subjected to constant body-fixed torque. However, due to the nonlinear nature of the problem, the discussion of this fundamental problem found in most engineering contexts[2–6] consists mainly of special cases such as axisymmetric and/or torque-free rotations.

More recent research resulted in exact and perturbation-based approximations for a wide variety of special cases. A perturbation approach to the arbitrary torqued motion of an asymmetric rigid body was suggested by Kraige and Junkins.[7] They formulated the problem using an Encke-type variation-of-parameters perturbation method about the analytical solution to the torque-free motion. Kraige and Skaar[8] provided comparison of computer execution times for these and two other motion prediction methods. Cochran et al.[9] presented an exact solution for the torque-free motion of a dual-spin spacecraft. A closed-form solution for the linearized rotational equations with traverse torques and a constant spin rate was studied by Larson and Likins.[10] Longuski,[11] Tsiotras and Longuski,[12,13] and Longuski and Tsiotras[14] developed analytical approximations for the motion of a near-symmetric rigid body subject to both constant and time-varying body-fixed moments about its three principal axes.

This paper draws heavily on the monograph by Leimanis[1] to address the problem of an asymmetric rigid body subject to constant body-fixed torques. Basic concepts of equilibrium manifolds, separatrices, and integrals of motions are used to generate new analytical as well as simulation results for constant torque along either the major, intermediate, or minor axis.

The main result of this paper can be perceived as follows. For the stability analysis of an asymmetric body subjected to constant body-fixed torque along one of its principal axes, a set of one-dimensional separatrix curves was plotted on a two-dimensional phase plane in Ref. 1. The coordinates used in the phase plane are rather physically nonintuitive, and the analysis is carried for one set of initial conditions at a time. The main contribution of this paper is the transition from a two-dimensional phase plane into a three-dimensional phase space for the purpose of stability analysis. The three-dimensional phase space coordinates are the components of the nondimensionalized angular velocity in the body coordinate system. The resulting coordinate system is identical to the one used in the stability analysis of a torque-free rotating body and therefore lends itself more readily to physical interpretation. The separatrices are plotted as two-dimensional surfaces in the three-dimensional phase space and capture all possible sets of initial conditions using only one plot.

The contributions of this paper are the following: 1) scaling of the equations of motion to eliminate their dependence on the inertia properties for the case of time-varying body-fixed torque; 2) for the case of constant body-fixed torque, nondimensionalization of the equations of motion to eliminate their dependence on both the inertia properties and the magnitude of the torque; 3) determination of the equilibrium manifolds for the nondimensional system; 4) derivation of the linearized equations of motion, the characteristic equation, and the stability properties of the nondimensional system; 5) evaluation of the integrals of motion and the two separatrix surfaces in a three-dimensional phase space for the case of a constant torque along the major/minor axis; and 6) evaluation of the integrals of motion and the two conventional separatrix surfaces in a three-dimensional phase space for the case of a constant torque along the intermediate axis. An extensive analysis of the values at the extrema of the various nondimensional angular velocity components along a periodic solution is also provided in the Appendix.

Equations of Motion

The rotational motion of a general rigid body under the influence of body-fixed torque is described by Euler's equations of motion of the form

$$I_1 \frac{d\omega_1}{dt} - (I_2 - I_3)\omega_2\omega_3 = M_1 \tag{1}$$

$$I_2 \frac{d\omega_2}{dt} - (I_3 - I_1)\omega_3\omega_1 = M_2 \tag{2}$$

$$I_3 \frac{d\omega_3}{dt} - (I_1 - I_2)\omega_1\omega_2 = M_3 \tag{3}$$

where I_1, I_2, and I_3 are the principal moments of inertia, $(\omega_1, \omega_2, \omega_3)$ is the angular velocity vector, and (M_1, M_2, M_3) is the time-varying body-fixed torque vector. Without loss of generality, it is assumed that $I_1 > I_2 > I_3$.

Defining

$$k_1 \equiv \frac{I_2 - I_3}{I_1}, \qquad k_2 \equiv \frac{I_1 - I_3}{I_2}, \qquad k_3 \equiv \frac{I_1 - I_2}{I_3}$$

$$k \equiv k_1 k_2 k_3, \qquad \tau \equiv \sqrt{k}\, t, \qquad u_i \equiv \frac{M_i}{I_i} \tag{4}$$

$$x_i \equiv \frac{\omega_i}{\sqrt{k_i}}, \qquad \mu_i \equiv \frac{1}{\sqrt{k}}\left(\frac{u_i}{\sqrt{k_i}}\right) \qquad (i = 1, 2, 3)$$

one can eliminate the dependence of Eqs. (1–3) on the inertia properties of the rotating body and write them as

$$\frac{dx_1}{d\tau} - x_2 x_3 = \mu_1 \tag{5}$$

Received Aug. 27, 1996; revision received April 15, 1997; accepted for publication April 16, 1997.

*Research Scientist, Aerospace Research Center. Senior Member AIAA.
†Professor, Department of Mechanical and Aerospace Engineering. Associate Fellow AIAA.

Table 1 Linear stability of various equilibrium points

Case	Equilibrium	Characteristic equation	Stability	Torque	Remarks
1	$(0, 0, 0)$	$s^3 = 0$	Unstable	$(0, 0, 0)$	None
2	$(X_1, 0, 0)$	$s(s^2 + X_1^2) = 0$	Stable	$(0, 0, 0)$	None
3	$(0, X_2, 0)$	$s(s^2 - X_2^2) = 0$	Unstable	$(0, 0, 0)$	None
4	$(0, 0, X_3)$	$s(s^2 + X_3^2) = 0$	Stable	$(0, 0, 0)$	None
5	$(0, X_2, X_3)$	$s(s^2 + X_3^2 - X_2^2) = 0$	Stable for $\lvert X_2\rvert < \lvert X_3\rvert$	$(-\mu_1, 0, 0)$	$X_2X_3 = -\mu_1$, $\lVert\mu_1\rVert = 1$
6	$(X_1, 0, X_3)$	$s(s^2 + X_1^2 + X_3^2) = 0$	Stable	$(0, \mu_2, 0)$	$X_1X_3 = \mu_2$, $\lVert\mu_2\rVert = 1$
7	$(X_1, X_2, 0)$	$s(s^2 + X_1^2 - X_2^2) = 0$	Stable for $\lvert X_1\rvert > \lvert X_2\rvert$	$(0, 0, -\mu_3)$	$X_1X_2 = -\mu_3$, $\lVert\mu_3\rVert = 1$
8	(X_1, X_2, X_3)	Eq. (18)	Unstable	(μ_1, μ_2, μ_3)	$\mu_1\mu_2\mu_3 > 0$, $\lVert\mu\rVert = 1$

$$\frac{dx_2}{d\tau} + x_3x_1 = \mu_2 \tag{6}$$

$$\frac{dx_3}{d\tau} - x_1x_2 = \mu_3 \tag{7}$$

where τ is the scaled time and (x_1, x_2, x_3) and (μ_1, μ_2, μ_3) are the scaled angular velocity and the scaled constant torque vectors, respectively.

For the case of constant body-fixed torque vector, one can further eliminate the dependence of Eqs. (1–3) on the magnitude of the torque vector (M_1, M_2, M_3).

Introducing

$$u \equiv \frac{\sqrt{k_2k_3u_1^2 + k_1k_3u_2^2 + k_1k_2u_3^2}}{k} \tag{8}$$

and using it to redefine τ, (x_1, x_2, x_3), and (μ_1, μ_2, μ_3) as

$$\tau \equiv \sqrt{ku}\, t, \qquad \mu_i \equiv (1/u\sqrt{k})(u_i/\sqrt{k_i})$$
$$x_i \equiv \omega_i/\sqrt{uk_i} \qquad (i = 1, 2, 3) \tag{9}$$

one can write Eqs. (1–3) as

$$\frac{dx_1}{d\tau} - x_2x_3 = \mu_1 \tag{10}$$

$$\frac{dx_2}{d\tau} + x_3x_1 = \mu_2 \tag{11}$$

$$\frac{dx_3}{d\tau} - x_1x_2 = \mu_3 \tag{12}$$

where τ is the nondimensional time and (x_1, x_2, x_3) and (μ_1, μ_2, μ_3) are the nondimensional angular velocity and the nondimensional constant torque vectors, respectively, and we have

$$\mu_1^2 + \mu_2^2 + \mu_3^2 = 1 \tag{13}$$

which can be easily verified using Eq. (9). The rest of this paper uses the nondimensional quantities τ, (x_1, x_2, x_3), and (μ_1, μ_2, μ_3) as defined in Eq. (9).

The equations of motion at steady state become

$$(-X_2X_3, X_1X_3, -X_1X_2) = (\mu_1, \mu_2, \mu_3) \tag{14}$$

where (X_1, X_2, X_3) is the equilibrium point. Equation (14) yields $\mu_1\mu_2\mu_3 = X_1^2X_2^2X_3^2$, which indicates that equilibrium points exist if and only if $\mu_1\mu_2\mu_3 > 0$ (only if $\mu_1\mu_2\mu_3 \geq 0$). Given a nondimensional torque vector (μ_1, μ_2, μ_3) with $\mu_1\mu_2\mu_3 \geq 0$, there exist eight equilibrium points given by

$$(X_1, X_2, X_3) = \left(\pm\sqrt{\mu_2\mu_3/\mu_1}, \pm\sqrt{\mu_3\mu_1/\mu_2}, \pm\sqrt{\mu_1\mu_2/\mu_3}\right) \tag{15}$$

Defining the angular velocity perturbation terms as

$$\Delta x_i \equiv x_i - X_i \qquad (i = 1, 2, 3) \tag{16}$$

and keeping μ_i constant, one can obtain the linearized equations of motion as

$$\frac{d}{d\tau}\begin{bmatrix}\Delta x_1\\ \Delta x_2\\ \Delta x_2\end{bmatrix} = \begin{bmatrix}0 & X_3 & X_2\\ -X_3 & 0 & -X_1\\ X_2 & X_1 & 0\end{bmatrix}\begin{bmatrix}\Delta x_1\\ \Delta x_2\\ \Delta x_2\end{bmatrix} \tag{17}$$

The characteristic equation is then obtained as

$$\lambda^3 + \left(X_1^2 - X_2^2 + X_3^2\right)\lambda + 2X_1X_2X_3 = 0 \tag{18}$$

An exhaustive listing of all of the possible combinations of constant torque, the angular velocities, and the resulting conditions for existence and stability of the roots of the characteristic equation (18) is provided in Table 1.

Constant Torque Along the Major/Minor Axis

Major Axis

For a positive constant torque acting along the major axis, Eqs. (10–12) simply become

$$\frac{dx_1}{d\tau} - x_2x_3 = 1 \tag{19}$$

$$\frac{dx_2}{d\tau} + x_3x_1 = 0 \tag{20}$$

$$\frac{dx_3}{d\tau} - x_1x_2 = 0 \tag{21}$$

The equilibrium points of the system described by Eqs. (19–21) constitute a hyperbola of the form $-X_2X_3 = 1$ and are stable when $|X_3| > 1$ and unstable when $|X_2| > 1$. Introducing a new variable θ_1 such that[1]

$$\theta_1(\tau) = \int_0^\tau x_1(\xi)\, d\xi \tag{22}$$

or $d\theta_1/d\tau = x_1(\tau)$ with $\theta_1(0) = 0$, one can write Eqs. (19–21) as

$$\frac{d^2\theta_1}{d\tau^2} - x_2x_3 = 1 \tag{23}$$

$$\frac{dx_2}{d\theta_1} + x_3 = 0 \tag{24}$$

$$\frac{dx_3}{d\theta_1} - x_2 = 0 \tag{25}$$

The solution to Eqs. (24) and (25) is given by

$$x_2 = A\cos(\theta_1 + \phi) \tag{26}$$

$$x_3 = A\sin(\theta_1 + \phi) \tag{27}$$

where $A = \sqrt{[x_2^2(0) + x_3^2(0)]}$ and $\phi \equiv \tan^{-1}[x_3(0)/x_2(0)]$ for $(|\phi| \leq \pi)$, and we have

$$x_2^2 + x_3^2 = A^2 \tag{28}$$

Depending on the range of θ_1, the projection of the tip of the nondimensional angular velocity vector (x_1, x_2, x_3) constitutes a complete circle or a portion of a circle on the (x_2, x_3) plane. The radius A of this circle (or portion of a circle) depends only on the initial value of the second and third components of the nondimensional angular velocity and is, therefore, the first integral of the motion of a rotating rigid body. Substituting Eqs. (26) and (27) into Eq. (23), we obtain

$$\frac{d^2\theta_1}{d\tau^2} - \frac{A^2}{2}\sin 2(\theta_1 + \phi) = 1 \tag{29}$$

Defining

$$\theta \equiv 2(\theta_1 + \phi) \tag{30}$$

Eq. (29) can be rewritten as

$$\frac{d^2\theta}{d\tau^2} - A^2 \sin\theta = 2 \tag{31}$$

At the equilibrium angle θ^*, we have $\sin\theta^* = -2/A^2$. Clearly no equilibrium point exists for $A < \sqrt{2}$. To study the stability properties of the system for the case when $A \geq \sqrt{2}$, introduce a new variable $x \equiv d\theta/d\tau$ and rewrite Eq. (31) in the (θ, x) phase plane representation as

$$\frac{d\theta}{d\tau} = x \tag{32}$$

$$\frac{dx}{d\tau} = A^2 \sin\theta + 2 \tag{33}$$

Dividing Eq. (33) by Eq. (32) to obtain

$$\frac{dx}{d\theta} = \frac{A^2 \sin\theta + 2}{x} \tag{34}$$

and noting that the first integral of the motion A remains constant for a given trajectory, one can separate variables and integrate Eq. (34) to obtain

$$(x^2/2) + A^2\cos\theta - 2\theta = E \tag{35}$$

where the nondimensional energy constant E is the second integral of the motion of the system. Given a value of the first integral of the motion A, one can use Eq. (35) to generate contour plots of the second integral of motion E on the (θ, x) phase plane. Such a contour plot is depicted in Fig. 1 for $A = 3$, where each one of either the dashed or the solid lines contours corresponds to a trajectory with constant levels of E. When $A > \sqrt{2}$, we have an infinite number of stable (centers +) and unstable (saddles ○) equilibrium points that are intermittently positioned along the θ axis in the (θ, x) phase

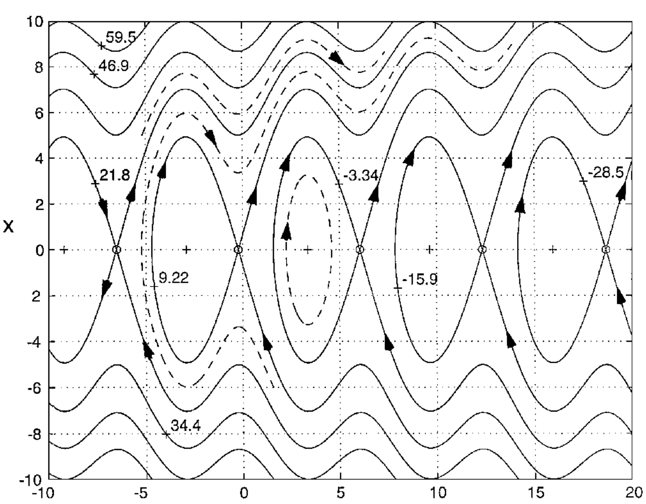

Fig. 1 Separatrices and typical bounded and unbounded trajectories for a constant major axis torque with $[x_1(0), x_2(0), x_3(0)]$ = (1.5, 0, 3), $[x_1(0), x_2(0), x_3(0)]$ = (−3, 2.12, 2.12), and $[x_1(0), x_2(0), x_3(0)]$ = (2.5, −1.8, 2.4).

plane. The first equilibrium point to the left of the origin in the (θ, x) phase plane is given by $(\theta^*, x^*) = [\sin^{-1}(-2/A^2), 0]$, where $|\sin^{-1}\psi| \leq \pi/2$ for all ψ. The saddle points are located at $\theta^* \pm 2n\pi$, whereas the center points are located at $\pi - \theta^* \pm 2n\pi$, $n = 1, 2, 3, \ldots, \infty$. The energy constant associated with a saddle point θ_S is given by

$$E_S = A^2\cos\theta_S - 2\theta_S \tag{36}$$

and the equation of the separatrix passing through θ_S is

$$(x^2/2) + A^2\cos\theta - 2\theta = E_S \tag{37}$$

or

$$x = \pm\sqrt{2}\,A\sqrt{\cos\theta_S - \cos\theta + (\theta_S - \theta)\sin\theta_S} \tag{38}$$

Recalling that $\theta(0) = 2\phi$ and that $|\phi| \leq \pi$, the only two separatrices of interest for stability analysis are the left separatrix, passing through the left saddle point at $\theta_{S_L} = \theta^*$ and encircling the left center at $\theta_{C_L} = -\theta^* - \pi$, and the right separatrix, passing through the right saddle point at $\theta_{S_R} = \theta^* + 2\pi$ and encircling the right center at $\theta_{C_R} = -\theta^* + \pi$. Figure 2 depicts the left and right separatrices for $A = \sqrt{(9.25)}$. Also shown are θ_{V_L} and θ_{V_R}, which are the vertical crossing associated with the left and right separatrices, respectively. Substituting $x = 2x_1$, $\cos\theta = (1 - \tan^2\theta/2)/(1 + \tan^2\theta/2) = (x_2^2 - x_3^2)/A^2$, and $\theta = 2\tan^{-1}(x_3/x_2)$ into Eq. (35) yields

$$2x_1^2 + x_2^2 - x_3^2 - 4\tan^{-1}(x_3/x_2) = E \tag{39}$$

which is the three-dimensional representation of a trajectory with energy constant E.

Noting that $\cos\theta_S = \sqrt{(A^4 - 4)}/A^2$, one can manipulate Eq. (37) to obtain

$$2x_1^2 + x_2^2 - x_3^2 - \sqrt{\left(x_2^2 + x_3^2\right)^2 - 4}$$
$$-2\sin^{-1}\frac{2}{x_2^2 + x_3^2} - 4\tan^{-1}\frac{x_3}{x_2} = 0 \tag{40}$$

which is a three-dimensional representation of the left separatrix. The right separatrix can be obtained by changing the right-hand side of Eq. (40) from 0 to -4π.

Figure 3 provides a three-dimensional depiction of the left and right separatrix surfaces in the (x_1, x_2, x_3) phase space. The two surfaces partition the (x_1, x_2, x_3) space into three infinite regions consisting of two stable regions that are separated by an unstable region. A motion with initial conditions inside one of these regions will remain confined to that region. Any motion with initial conditions in the unstable domain will result in a spin-up maneuver, whereas any motion with initial conditions in either one of the stable regions will result in a closed and bounded trajectory confined to

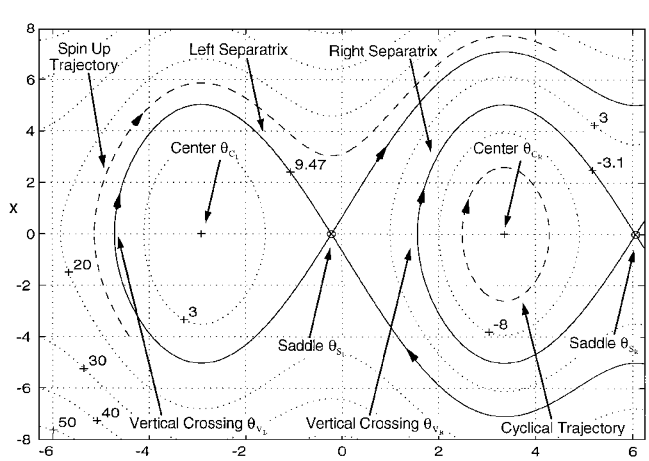

Fig. 2 Left and right separatrices and typical bounded and unbounded trajectories for a constant major axis torque with $[x_1(0), x_2(0), x_3(0)]$ = (1, 0.5, 3) and $[x_1(0), x_2(0), x_3(0)]$ = (−2, −1.8, −2.45).

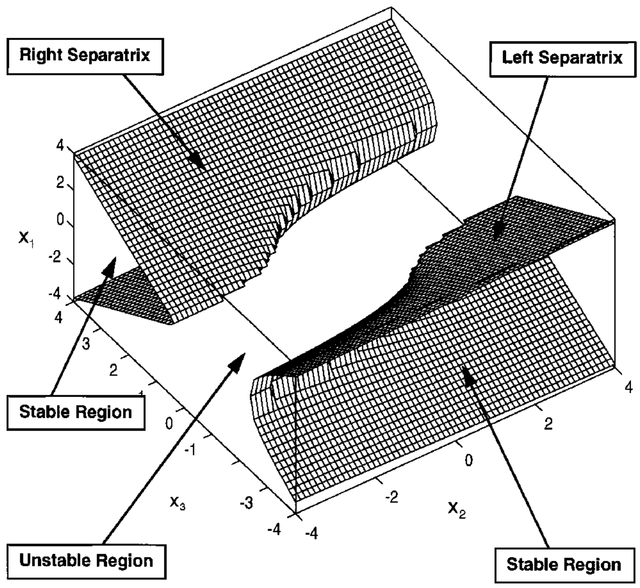

Fig. 3 Left and right separatrix surfaces for a constant major axis torque.

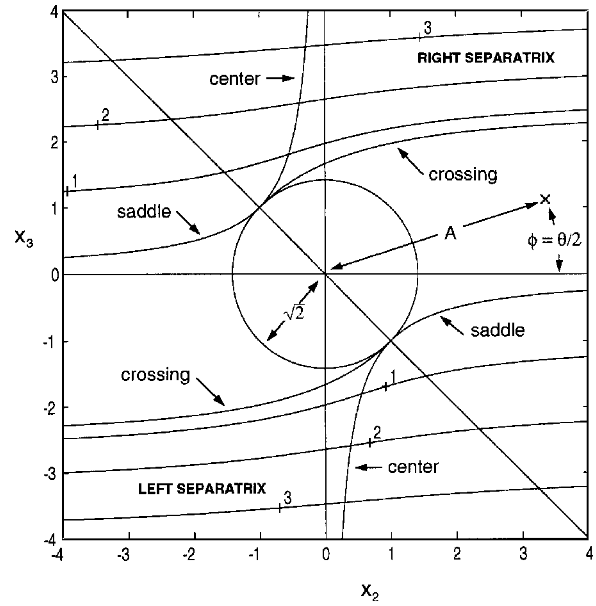

Fig. 4 Contour plots of $x_1(A, \phi)$ of the left and right separatrix surfaces for a constant major axis torque.

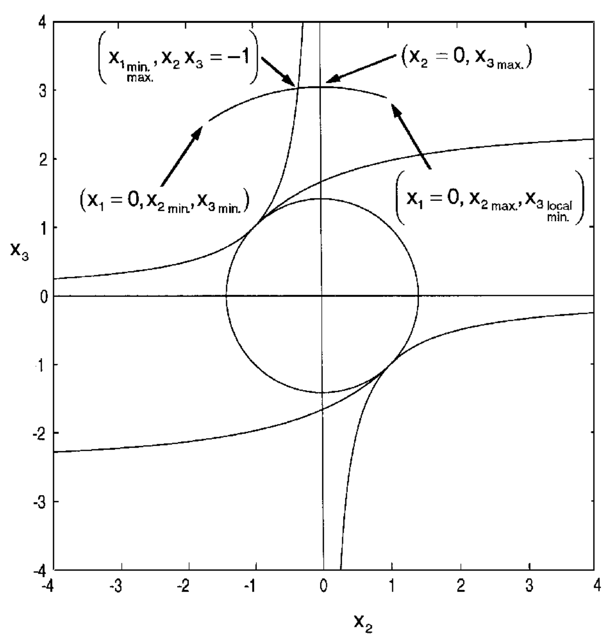

Fig. 5 Projection of a typical stable trajectory on the (x_2, x_3) for a constant major axis torque with $[x_1(0), x_2(0), x_3(0)] = (1, 0.5, 3)$.

that region and rotating about its corresponding center. For example, a trajectory in the right stable region will rotate about a center at

$$\left(0, -\sqrt{\frac{A^2 - \sqrt{A^4 - 4}}{2}}, \sqrt{\frac{A^2 + \sqrt{A^4 - 4}}{2}}\right)$$

The projection of the tip of the nondimensional angular velocity vector (x_1, x_2, x_3) on the (x_2, x_3) plane constitutes a complete circle for initial conditions inside the unstable region and a portion of a circle for initial conditions inside either one of the stable regions. The radius A of this circle can be arbitrarily large, resulting in either a stable or an unstable motion. Note that any trajectory with initial conditions $[x_1(0) < 0, x_2(0), x_3(0)]$ in the lower unstable domain will cross the part of the (x_2, x_3) plane contained in the unstable region, i.e., the gap between the two separatrix surfaces, at a distance of $A = \sqrt{[x_2^2(0) + x_3^2(0)]}$ from the origin of the (x_1, x_2, x_3) coordinate system. Because A can be arbitrarily large, the gap between the two separatrix surfaces extends to $\pm\infty$ along the x_2 axis. It is also observed that all of the equilibrium points inside the stable domain, shown to be Lyapunov stable for the linearized system, are Lyapunov stable for the nonlinear system.

Figure 4 is a contour plot of the top half $(x_1 > 0, x_2, x_3)$ of the left and right separatrix surfaces depicted in Fig. 3. Also depicted are 1) the cylindrical coordinates $A = \sqrt{[x_2^2(0) + x_3^2(0)]}$ and $\phi = \tan^{-1}[x_3(0)/x_2(0)]$, 2) the circle $A = \sqrt{2}$ inside of which there do not exist any equilibrium points, 3) the two branches of the hyperbola $x_2 x_3 = -1$, which are the locus of all of the equilibrium points of the system, and 4) the line $x_2 + x_3 = 0$, which partitions the two branches of the hyperbola $x_2 x_3 = -1$ into Lyapunov stable and unstable domains. The projection of a typical stable trajectory initiated from $[x_1(0), x_2(0), x_3(0)] = (1, 0.5, 3)$ on the (x_2, x_3) plane is shown in Fig. 5. Because the trajectory is in the stable region enclosed by the right separatrix surface, its projection on the (x_2, x_3) plane constitutes a portion of a circle with a radius of $\sqrt{(9.25)} = 3.04$.

The intersection between the two separatrix surfaces and the (x_2, x_3) plane can be found from Eq. (38) to be the solution to the transcendental equations given by

$$\cos\theta_S - \cos\theta + (\theta_S - \theta)\sin\theta_S = 0 \tag{41}$$

One obvious solution to Eq. (41) is $\theta_S = \theta$. This solutions yield

$$\sin\theta_S = \sin\theta = \frac{2\tan\theta/2}{1 + \tan^2\theta/2} = \frac{2x_2x_3}{x_2^2 + x_3^2} \tag{42}$$

Because $\sin\theta_S = -2/(x_2^2 + x_3^2)$, the only way to satisfy Eq. (42) is to choose $x_2 x_3 = -1$. The part of the hyperbola $x_2 x_3 = -1(|x_2| > 1)$ corresponding to the locus of the unstable equilibrium points lies, therefore, on the intersection between the left and right separatrix surfaces and the (x_2, x_3) plane. When $(|x_3| > 1)$, the intersection between the two separatrix surfaces and the (x_2, x_3) plane is found by solving Eq. (41) numerically.

Recall that each of the separatrix phase plane plots, such as Fig. 2, was constructed for a single value of A, whereas Figs. 3 and 4 represent all possible values of $0 \le A \le \infty$. The saddle, center, and vertical crossing points associated with the left and right separatrices of Fig. 2 correspond to the intersection of a circle of radius $A = \sqrt{(9.25)}$ with the saddle, center, and vertical crossing curves depicted in Fig. 4. When $A = \sqrt{2}$, the saddle, center, and vertical crossing associated with the left separatrix surface all collapse into one point at $(x_1, x_2, x_3) = (0, 1, -1)$, whereas the saddle, center, and vertical crossing associated with the right separatrix surface all collapse into $(x_1, x_2, x_3) = (0, -1, 1)$. Therefore, the saddle, center, and crossing curves depicted in Fig. 4 can be constructed by starting with $A = \sqrt{2}$ in Fig. 2 and tracing the polar coordinates $(A, \phi = \theta/2)$ spanned by the saddle, center, and crossing points as A is increased. A motion initiated from the separatrix surface will remain confined to that surface and will converge asymptotically to the equilibrium point in the intersection of $x_2^2 + x_3^2 = A^2$ with the unstable branch of the hyperbola $x_2x_3 = -1$, contained in that surface. For example, motion started from the right separatrix will converge to

$$(x_1, x_2, x_3) = \left(0, -\sqrt{\frac{A^2 + \sqrt{A^4 - 4}}{2}}, \sqrt{\frac{A^2 - \sqrt{A^4 - 4}}{2}}\right)$$

Analytical expressions for the extrema of the various nondimensional angular velocity components along a periodic solution for the case of constant major axis torque are given in Table A1 in the Appendix.

Minor Axis

Because of the particular form of the nondimensional Euler equations (10–12), the solution for the case of a constant torque acting along the minor axis can be obtained by interchanging the indices 3 and 1 in the preceding derivation.

Constant Torque Along the Intermediate Axis

For the case of a positive constant torque acting along the intermediate axis, Eqs. (10–12) yield

$$\frac{dx_1}{d\tau} - x_2x_3 = 0 \tag{43}$$

$$\frac{dx_2}{d\tau} + x_3x_1 = 1 \tag{44}$$

$$\frac{dx_3}{d\tau} - x_1x_2 = 0 \tag{45}$$

In this case, the equilibrium points of the system constitute a hyperbola of the form

$$X_1X_3 = 1 \tag{46}$$

This hyperbola corresponds to case 6 in Table 1. Therefore the equilibrium points of the linearized system associated with the nonlinear system of Eqs. (43–45) are Lyapunov stable. Introducing a new variable θ_2 such that[1]

$$\theta_2(\tau) = \int_0^\tau x_2(\xi)\, d\xi \tag{47}$$

or $d\theta_2/d\tau = x_2(\tau)$ and $\theta_2(0) = 0$, and noting that $d/d\tau = x_2\, d/d\theta_2$, one can write Eqs. (43–45) as

$$\frac{dx_1}{d\theta_2} - x_3 = 0 \tag{48}$$

$$\frac{d^2\theta_2}{d\tau^2} + x_1x_3 = 1 \tag{49}$$

$$\frac{dx_3}{d\theta_2} - x_1 = 0 \tag{50}$$

The solution to Eqs. (48) and (50) is given by

$$x_1 = x_1(0)\cosh\theta_2 + x_3(0)\sinh\theta_2 \tag{51}$$

$$x_3 = x_1(0)\sinh\theta_2 + x_3(0)\cosh\theta_2 \tag{52}$$

This solution satisfies

$$x_1^2 - x_3^2 = x_1^2(0) - x_3^2(0) = \text{const} \tag{53}$$

The projection of the nondimensional angular velocity vector x on the (x_1, x_3) plane is confined to the hyperbola of Eq. (53) and is therefore determined by its initial conditions. Substitution of Eqs. (51) and (52) into Eq. (49) yields

$$\frac{d^2\theta_2}{d\tau^2} = 1 - A\sinh 2\theta_2 - B\cosh 2\theta_2 \tag{54}$$

where

$$A = \frac{x_1^2(0) + x_3^2(0)}{2}, \qquad B = x_1(0)x_3(0) \tag{55}$$

Trajectories with $|x_1(0)| \neq |x_3(0)|$

In this case $A > B$, and Eq. (54) can be manipulated to obtain

$$\frac{d^2\theta_2}{d\tau^2} = 1 - \sqrt{A^2 - B^2}\,\sinh(2\theta_2 + \phi) \tag{56}$$

where $\phi = \tanh^{-1}(B/A)$.

Defining

$$\theta \equiv 2\theta_2 + \phi, \qquad C \equiv \frac{\left|x_1^2(0) - x_3^2(0)\right|}{2} \tag{57}$$

and noting that

$$A^2 = B^2 + C^2 \tag{58}$$

one can rewrite Eq. (56) as

$$\frac{d^2\theta}{d\tau^2} = 2 - 2C\sinh\theta \tag{59}$$

Also in light of Eq. (53), C is the first integral of the motion. The system described by Eq. (59) is conservative, and its equilibrium point is given by

$$\theta^* \equiv \sinh^{-1}(C^{-1}) \tag{60}$$

Because $-\infty < \sinh x < \infty$, every set of initial conditions $[x_1(0), x_3(0)]$ has associated with it only one equilibrium point. Equation (60) defines, therefore, a unique equilibrium point per set of initial conditions. Furthermore, if our trajectory is started at an equilibrium point of the system, we have $\theta^* = \theta_2(\tau) = \theta_2(0) = \phi$, leading to

$$\frac{1}{C} = \sinh\phi = \frac{\tanh\phi}{\sqrt{1 - \tanh^2\phi}} = \frac{B}{C} \tag{61}$$

which implies

$$B = x_1(0)x_3(0) = X_1X_3 = 1 \tag{62}$$

and is in perfect agreement with Eq. (46). Because the right-hand side of Eq. (59) can be interpreted as representing a conservative force field, the system has an energy constant. To find this constant, rewrite Eq. (59) as

$$\frac{d\theta}{d\tau} = x \tag{63}$$

$$\frac{dx}{d\tau} = 2 - 2C\sinh\theta \tag{64}$$

Dividing Eq. (64) by Eq. (63) yields

$$\frac{dx}{d\theta} = \frac{2 - 2C\sinh\theta}{x} \tag{65}$$

Because C is the first integral of the motion, one can separate variables and integrate Eq. (64) to get

$$(x^2/2) + 2C\cosh\theta - 2\theta = E \tag{66}$$

where the nondimensional energy constant (not the energy) of the system E is the second integral of motion of the system. The nondimensional potential energy variable (not potential energy) of the system can be defined as

$$V = 2C\cosh\theta - 2\theta \tag{67}$$

Noting that

$$\frac{d^2V}{d\theta^2} = 2C\cosh\theta > 0 \tag{68}$$

one can easily conclude that the equilibrium point θ^* is stable. This means that every initial condition for $|x_1(0)| \neq |x_3(0)|$ forms a closed periodic trajectory of an oval shape about a unique Lyapunov stable equilibrium point.

Because any point on a trajectory can also be considered as a set of initial conditions for this trajectory, the relations $2C\cosh\theta(0) = 2C\cosh\phi = 2C/\sqrt{(1-\tanh^2\phi)} = x_1^2(0) + x_3^2(0)$ and $x = 2x_2$ enable us to write Eq. (66) as

$$x_1^2 + 2x_2^2 + x_3^2 - 2\tanh^{-1}\frac{2x_1x_3}{x_1^2 + x_3^2} = E \tag{69}$$

Equation (69) is a three-dimensional description of a closed trajectory with energy constant E. It is derived for the case of constant torque along the intermediate axis and with initial conditions satisfying $|x_1(0)| \neq |x_3(0)|$. Clearly, any motion initiated from this closed trajectory will remain confined to it.

A typical closed trajectory plot for the case of constant torque along the intermediate axis is shown in Fig. 6 for the initial condition of $x(0) = (1, 0.5, -0.5)$. Figure 7 is a projection of the curve depicted in Fig. 6 on the (x_1, x_3) plane. The motion trajectories are closed and encircle the locus $x_1x_3 = 1$ of equilibrium points. The projection of the trajectory on the (x_1, x_3) plane lies on the positive branch of the hyperbola $x_1^2 - x_3^2 = \frac{3}{4}$ and therefore does not cross the two separatrix surfaces $x_1 = x_3$ and $-x_3$. The separatrix surfaces depicted in Figs. 6 and 7 are identical to the separatrices for the torque-free case. They consist of two perpendicular planes that intersect on the x_2 axis and are rotated about it to form a 45-deg angle with the (x_1, x_2) and (x_2, x_3) planes. These two separatrix planes partition the (x_1, x_2, x_3) space into four distinct (and infinite) regions given by $x_1 > |x_3|$, $-x_1 > |x_3|$, $x_3 > |x_1|$, and $-x_3 > |x_1|$. In the two regions satisfying $|x_1| > |x_3|$, the (x_1, x_3) projection of the solution trajectory lies on the corresponding branch of the hyperbola $x_1^2 - x_3^2 = x_1^2(0) - x_3^2(0) = 2C > 0$, whereas in the two regions satisfying $|x_3| > |x_1|$, the (x_1, x_3) projection of the solution trajectory lies on the corresponding branch of the hyperbola $x_3^2 - x_1^2 = x_3^2(0) - x_1^2(0) = 2C > 0$. Analytical expressions for the extrema of the various nondimensional angular velocity components for the case of constant intermediate axis torque with $|x_1(0)| \neq |x_3(0)|$ are given in Table A2 in the Appendix.

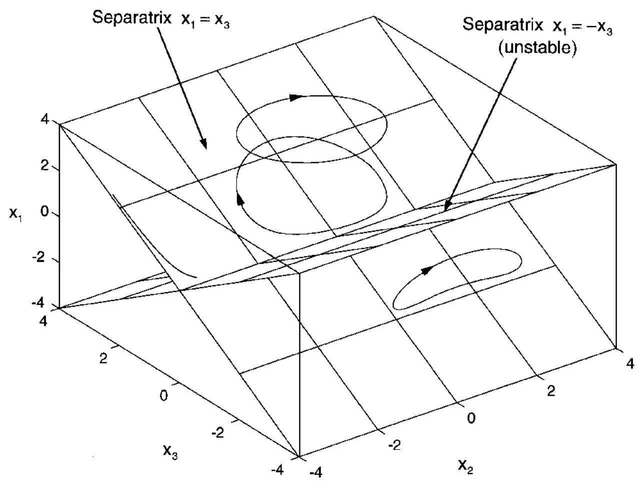

Fig. 6 Separatrix surfaces for constant intermediate axis torque with $[x_1(0), x_2(0), x_3(0)] = (1, 0.5, -0.5)$.

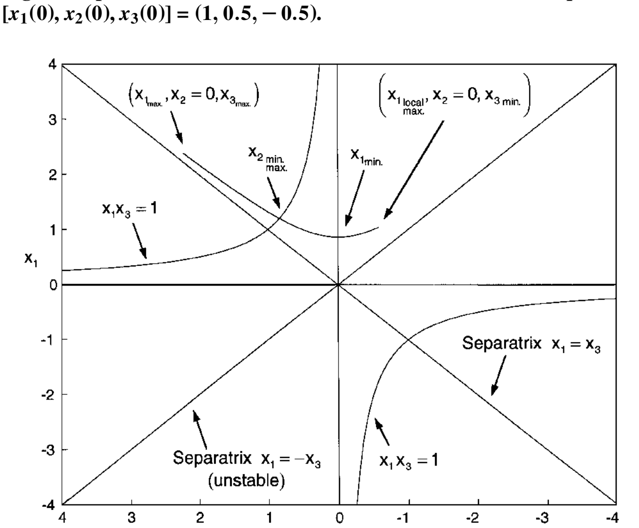

Fig. 7 Projection of the separatrix surfaces on the (x_1, x_3) plane for a constant intermediate axis torque with $[x_1(0), x_2(0), x_3(0)] = (1, 0.5, -0.5)$.

Stable Separatrix $x_1 = x_3$

The case $x_1(0) = x_3(0) = 0$ results in a pure spin up about the intermediate axis, as can be seen from Eqs. (43–45). When $x_1(0) = x_3(0) \neq 0$, Eqs. (51) and (52) yield

$$\left.\begin{aligned} x_1 &= x_1(0)e^{\theta_2} \\ x_3 &= x_3(0)e^{\theta_2} \end{aligned}\right\} \Rightarrow x_1 = x_3 \Rightarrow C = 0 \tag{70}$$

where C is the first integral of the motion. Because in this case we have $A = B$, Eq. (54) yields

$$\frac{d^2\theta_2}{d\tau^2} = 1 - Ae^{2\theta_2} \tag{71}$$

At equilibrium we have

$$x_1^* = x_1(0) = x_1(0)e^{\theta_2^*} \Rightarrow \theta_2^* = 0 \tag{72}$$

$$x_3^* = x_3(0) = x_3(0)e^{\theta_2^*} \Rightarrow \theta_2^* = 0 \tag{73}$$

which when combined with Eq. (55) yields

$$A = B = x_1(0)x_3(0) = X_1X_3 = 1 \tag{74}$$

Examination of Eqs. (70) reveals that any motion started from the surface $x_1(0) = x_3(0)$ will not change sign, i.e., depending on its initial conditions, it will remain in the upper or the lower part of this surface for all τ. Equation (71) can be rewritten as

$$\frac{d\theta_2}{d\tau} = x_2 \tag{75}$$

$$\frac{dx_2}{d\tau} = 1 - x_1^2(0)e^{2\theta_2} \tag{76}$$

Next divide Eq. (76) by Eq. (75) to get

$$\frac{dx_2}{d\theta_2} = \frac{1 - x_1^2(0)e^{2\theta_2}}{x_2} \tag{77}$$

which, after separation of variables and integration, yields

$$\left(x_1^2/2\right) + \left(x_2^2/2\right) - \ln x_1 = E \tag{78}$$

where the nondimensional energy constant (not the energy) of the system E is the second integral of motion of the system. Stability analysis similar to that performed for $x_1(0) \neq x_3(0)$ reveals that every set of initial conditions satisfying $x_1 = x_3 > 0$ results in a closed periodic solution of an oval shape that is confined to the plane $x_1 = x_3 > 0$ and encircles the equilibrium point (1, 0, 1) contained in this plane, whereas every set of initial conditions satisfying $x_1 = x_3 < 0$ results in a closed periodic solution of an oval shape that is confined to the plane $x_1 = x_3 < 0$ and encircles the equilibrium point (−1, 0, −1) contained in that plane. Analytical expressions for the extrema of the various nondimensional angular velocity components for the case of constant intermediate axis torque with $x_1 = x_3 > 0$ are given in Table A3 in the Appendix.

Unstable Separatrix $x_1 = -x_3$

When $x_1(0) = -x_3(0)$, Eqs. (51) and (52) yield

$$\left.\begin{aligned} x_1 &= x_1(0)e^{-\theta_2} \\ x_3 &= x_3(0)e^{-\theta_2} \end{aligned}\right\} \Rightarrow x_1 = -x_3 \tag{79}$$

Because in this case $A = -B$, Eq. (54) yields

$$\frac{d^2\theta_2}{d\tau^2} = 1 + Ae^{-2\theta_2} \tag{80}$$

Clearly in this case we have no equilibrium points. Further examination of Eq. (80) reveals that

$$\lim_{\tau\to\infty}\frac{\mathrm{d}^2\theta_2}{\mathrm{d}\tau^2} = 1 \Rightarrow \lim_{\tau\to\infty} x_2 = x_2(0) + \tau = \infty \Rightarrow \lim_{\tau\to\infty}\theta_2$$
$$= x_2(0)\tau + \tau^2/2 = \infty \tag{81}$$

Substitution of Eq. (81) into Eq. (79) yields

$$\lim_{\tau\to\infty} x_1 = \lim_{\tau\to\infty} x_3 = 0 \tag{82}$$

When $x_1(0) = -x_3(0)$, the result of a constant torque on the intermediate axis is a motion that rapidly converges to a pure spin-up maneuver about the intermediate axis with constant angular acceleration.

Torque About Major/Minor vs Intermediate Axes

The large contrasts between the characteristics of the trajectories corresponding to the major/minor axis torquing vs intermediate axis torquing are the result of the sign differences between the transformed nondimensional equations (23–25) for the major/minor axis torquing and those for the intermediate axis, Eqs. (48–50).

The difference in the trajectory characteristics between major/minor axis torquing and intermediate axis torquing is the result of the sign differences in their corresponding formulation of Eqs. (23–25) and Eqs. (48–50), respectively. These sign differences lead to the different linear homogeneous part of the equations of motion, resulting in the harmonic solution of Eqs. (26) and (27) for the major/minor axis torquing vs the hyperbolic solution of Eqs. (51) and (52) for the intermediate axis torquing. The (x_2, x_3) projection of the harmonic solution lies on a circle (or portion of a circle) whose radius is the first integral of motion of the major/minor axis torquing problem, whereas the (x_1, x_3) projection of the hyperbolic solution lies on a rectangular hyperbola whose traverse (and conjugate) axis is the first integral of motion of the intermediate axis torquing problem. Substitution of the harmonic and hyperbolic solutions into their respective (nonlinear, nonhomogeneous) differential equations (23) and (49) leads to the formulation of the second integral of motion, resulting in different stability properties for the two cases.

As discussed earlier, the major/minor axis torquing results in the left and right separatrices described in Figs. 3 and 4. The two curved separatrix surfaces do not intersect, and they partition the (x_1, x_2, x_3) state space into three infinite regions consisting of two stable regions that are separated by an unstable region. In the case of the intermediate axis torquing, the separatrix surfaces, depicted in Figs. 6 and 7, consist of two perpendicular planes that intersect on the x_2 axis and partition the (x_1, x_2, x_3) space into four distinct (and infinite) regions. A motion started from each of these regions results in a stable periodic trajectory confined to this region. The only instability in this case occurs for trajectories initiated from the unstable separatrix $x_1 = -x_3$, which rapidly converge to a spin-up maneuver about the intermediate axis.

Conclusions

The rotational dynamics of a general rigid body under the influence of constant body-fixed torque has been investigated. The main contribution of this paper is the transition from a two-dimensional phase plane into a three-dimensional phase space for the purpose of stability analysis of an asymmetric rigid body subjected to constant body-fixed torques.

Euler's rotational equations of motion were scaled to eliminate their dependence on the inertia for the case of time-varying body-fixed torque. For the case of constant body-fixed torque, these equations were further nondimensionalized to eliminate their dependence on both the inertia properties and the magnitude of the torque. Basic concepts such as equilibria, separatrices, and the integrals of motion associated with the trajectories of the system were brought from their two-dimensional phase plane form into a three-dimensional phase space representation. The nondimensional equations in conjunction with the new three-dimensional phase space graphics were utilized to illustrate those concepts and gain further understanding of their interrelationship in this fundamental yet highly nonlinear problem. Also provided is an extensive analysis of the extrema of the nondimensional periodic solution.

Appendix: Extremal Values Along Periodic Solutions to Euler's Rotational Equations

Torque Along the Major Axis

The extremal values taken by the nondimensional angular velocity component x_1, x_2, and x_3 along a closed trajectory in either one of the two stable regions for constant torque along the major axis can be obtained by manipulating Eqs. (19–21) as

$$\frac{\mathrm{d}x_1}{\mathrm{d}x_2} = -\frac{x_2x_3+1}{x_1x_3} = 0, \qquad \frac{\mathrm{d}x_2}{\mathrm{d}x_1} = -\frac{x_1x_3}{x_2x_3+1} = 0 \tag{A1}$$

$$\frac{\mathrm{d}x_1}{\mathrm{d}x_3} = \frac{x_2x_3+1}{x_1x_2} = 0, \qquad \frac{\mathrm{d}x_3}{\mathrm{d}x_1} = \frac{x_1x_2}{x_2x_3+1} = 0 \tag{A2}$$

$$\frac{\mathrm{d}x_2}{\mathrm{d}x_3} = -\frac{x_3}{x_2} = 0, \qquad \frac{\mathrm{d}x_3}{\mathrm{d}x_2} = -\frac{x_2}{x_3} = 0 \tag{A3}$$

A direct consequence of Eqs. (A1–A3) is that the extremal values of x_2 and x_3 will occur only in the intersection of the nondimensional angular velocity trajectory with either the (x_2, x_3) plane or the (x_1, x_3) plane, whereas the extremal values of x_1 will occur only in the intersection of this trajectory with the two surfaces $x_1x_3 = -1$. The extrema of x_1, x_2, and x_3 can be obtained by substituting Eqs. (A1–A3) into the equations for the constants of the motion A and E, given by Eqs. (28) and (39), and solving the resulting transcendental equations.

For example, one can calculate the extrema associated with initial conditions at $x(0) = (1, 0.5, 3)$ as depicted in Fig. 5. These initial conditions yield $E = -12.37$ and $A = 3.04$.

Equation (28) implies

$$x_2 = \pm\sqrt{A^2 - x_3^2} \qquad \text{and} \qquad x_3 = \pm\sqrt{A^2 - x_2^2} \tag{A4}$$

Substitution of Eqs. (A4) into Eq. (39) yields

$$2x_1^2 + 2x_2^2 \pm 4\tan^{-1}\frac{\sqrt{A^2 - x_2^2}}{x_2} = E \pm A^2 + 4n\pi \qquad n = 0, \pm 1 \tag{A5}$$

$$2x_1^2 - 2x_3^2 \pm 4\tan^{-1}\frac{x_3}{\sqrt{A^2 - x_3^2}} = E \pm A^2 + 4n\pi \qquad n = 0, \pm 1 \tag{A6}$$

The conditions for the extrema of x_1 are given by

$$x_2x_3 = -1 \tag{A7}$$

Substitution of Eq. (A7) into Eq. (28) yields

$$x_2 = -\sqrt{\frac{A^2 - \sqrt{A^4 - 4}}{2}} = -0.33 \tag{A8}$$

$$x_3 = \sqrt{\frac{A^2 + \sqrt{A^4 - 4}}{2}} = 3.02 \tag{A9}$$

and substitution of Eqs. (A8) and (A9) into Eq. (39) yields

$$x_1 = \pm\sqrt{\frac{E + 4\pi + \sqrt{A^4 - 4}}{2} - 2\tan^{-1}\frac{A^2 + \sqrt{A^4 - 4}}{2}} = \pm 1.30 \tag{A10}$$

These results are in good agreement with the numerical simulation results shown in Fig. 5.

The extrema of x_2 occur at the intersection of the nondimensional angular velocity trajectory with the (x_2, x_3) plane at $x_1 = 0$. Substitution of $x_1 = 0$ into Eq. (A5) yields $(x_1, x_2, x_3) = (0, -1.65, 2.55)$, which is a solution to $2x_2^2 - 4\tan^{-1}\{\sqrt{[(A/x_2)^2 - 1]}\} = E + A^2$ and $x_3 = \sqrt{(A^2 - x_2^2)}$, and $(x_1, x_2, x_3) = (0, 0.97, 2.88)$, which is a solution to $2x_2^2 - 4\tan^{-1}\{\sqrt{[(A/x_2)^2 - 1]}\} = E + A^2 + 4\pi$ and

Table A1 Formulation and numerical values of the extrema of x_1, x_2, and x_3 for $\mu = (1, 0, 0)$ in Fig. 5

Item	Analytical expression	Numerical value
General	$A = \sqrt{x_2^2(0) + x_3^2(0)}$	$x(0) = (1, 0.5, 3)$
	$E = 2x_1^2(0) + x_2^2(0) - x_3^2(0) - 4\tan^{-1}\left[\frac{x_3(0)}{x_2(0)}\right]$	$A = 3.041$, $E = -12.373$
$x_{1_{\max}}, x_{1_{\min}}$	$x_1 = \pm\sqrt{\frac{E + 4\pi + \sqrt{A^4 - 4}}{2} - 2\tan^{-1}\frac{A^2 + \sqrt{A^4 - 4}}{2}}$	$x = (\pm 1.30, -0.33, 3.02)$
	$x_2 = -\sqrt{\frac{A^2 - \sqrt{A^4 - 4}}{2}}, \quad x_3 = \sqrt{\frac{A^2 + \sqrt{A^4 - 4}}{2}}$	
$x_{2_{\max}}, x_{3_{\text{local min}}}$	$x_1 = 0, \quad 2x_2^2 + 4\tan^{-1}\left(\frac{\sqrt{A^2 - x_2^2}}{x_2}\right) = E + A^2 + 4n\pi$	$x = (0, 0.97, 2.88)$, $n = 0$
$x_{2_{\min}}, x_{3_{\min}}$	$n = 0, \pm 1, \quad x_3 = \sqrt{A^2 - x_2^2}$	$x = (0, -1.65, 2.44)$, $n = 1$
$x_{3_{\max}}$	$x_1 = \pm\sqrt{\frac{E + A^2 + 2\pi}{2}}, \quad x_2 = 0, \quad x_3 = A$	$x = (\pm 1.26, 0, 3.04)$

Table A2 Formulation and numerical values of the extrema of x_1, x_2, and x_3 for $\mu = (0, 1, 0)$ in Figs. 6 and 7

Item	Analytical expression	Numerical value
General	$C = \frac{\left\lvert x_1^2(0) - x_3^2(0)\right\rvert}{2}$	$x(0) = (1, 0.5, -0.5)$
	$E = x_1^2(0) + 2x_2^2(0) + x_3^2(0) - 2\tanh\left\{\frac{2x_1(0)x_3(0)}{x_1^2(0) + x_3^2(0)}\right\}$	$E = 3.94$, $C = \frac{3}{8}$
$x_{1_{\text{local max}}}, x_{3_{\min}}$	$x_3^2 - \tanh^{-1}\left\{\frac{\sqrt{x_3^2 + 2C}}{x_3^2 + 2C}x_3\right\} + C - \frac{E}{2} = 0$	$x = (1.04, 0, -0.58)$
$x_{1_{\max}}, x_{3_{\max}}$	$x_2 = 0, \quad x_1 = \sqrt{x_3^2 + 2C}$	$x = (2.39, 0, 2.22)$
$x_{2_{\max}}, x_{2_{\min}}$	$x_1 = \sqrt{\sqrt{C^2 + 1} + C}, \quad x_3 = \sqrt{\sqrt{C^2 + 1} - C}$	$x = (1.20, \pm 1.62, 0.83)$
	$x_2 = \pm\sqrt{-\sqrt{C^2 + 1} + \tanh^{-1}\left(\frac{1}{\sqrt{C^2 + 1}}\right) + \frac{E}{2}}$	
$x_{1_{\min}}$	$x_1 = \sqrt{2C}, \quad x_2 = \pm\sqrt{\frac{E}{2} - C}, \quad x_3 = 0$	$x = (0.87, \pm 1.26, 0)$

Table A3 Formulation and numerical values of the extrema of x_1, x_2, and x_3 for $\mu = (0, 1, 0)$ and $x_1(0) = x_3(0) \neq 0$

Item	Analytical expression	Numerical value
General	$x_1 = x_3, \quad E = \frac{x_1^2(0) + x_2^2(0) - \ln x_1^2(0)}{2}$	$x(0) = (2, 1, 2)$, $E = 1.8069$
$x_{1_{\min}}, x_{1_{\max}}$	$\frac{x_1^2}{2} - \ln x_1 = E, \quad x_2 = 0, \quad x_3 = x_1$	$x = (0.17, 0, 0.17)$, $x = (2.30, 0, 2.30)$
$x_{2_{\min}}, x_{2_{\max}}$	$x_1 = 1, \quad x_2 = \pm\sqrt{2E - 1}, \quad x_3 = 1$	$x = (1, \pm 1.62, 1)$

$x_3 = \sqrt{(A^2 - x_2^2)}$. The point $(0, -1.65, 2.55)$ is a minimum for both x_2, and x_3, whereas $(0, 0.97, 2.88)$ is a maximum for x_2 and a local minimum for x_3. These points can be obtained by using Eq. (A6) instead of Eq. (A5).

The maximum value of x_3 occurs at the intersection of the nondimensional angular velocity trajectory with the (x_1, x_3) plane. For this case, Eqs. (A4) and (A5) yield $(x_1, x_2, x_3) = (\pm 1.26, 0, 3.04)$, which is a solution to $x_1 = \pm\sqrt{[(E + A^2 + 2\pi)/2]}$ and $x_3 = A$. These results are in good agreement with Fig. 5. The numerical results pertaining to Fig. 5 are summarized in Table A1.

Torque Along the Intermediate Axis

For the case of constant torque acting along the intermediate axis, the extremal values taken by x_2 and x_3 along a closed trajectory satisfying $|x_1| \neq |x_3|$ can be obtained similarly to the analysis of the case of a constant torque acting along the principal axis. The results of such analysis are summarized in Table A2 for Figs. 6 and 7. The extremal values taken by $x_1 = x_3$ and x_2 along a closed trajectory are summarized in Table A3 for a trajectory with initial conditions at $\boldsymbol{x}(0) = (2, 1, 2)$. Note that $x_{2_{\min}}$ and $x_{2_{\max}}$ occur when $(x_1, x_3) = (1, 1)$. Because this point resides on the equilibrium locus $x_1 x_3 = 1$, one can easily conclude that, as in the case of $x_1(0) \neq x_3(0)$, the two extrema for x_2 are located in the intersection points of the trajectory with the surface $x_1 x_3 = 1$.

One can therefore conclude that, as in the case of $x_1(0) \neq x_3(0)$, the two extrema of $x_1 = x_3$ are located at the intersection of the angular velocity trajectory with the plane $x_2 = 0$, whereas the two extrema for x_2 are located in the intersection points of the trajectory with the surface $x_1 x_3 = 1$.

References

[1]Leimanis, E., *The General Problem of the Motion of Coupled Rigid Bodies About a Fixed Point*, Vol. 7, Springer–Verlag, New York, 1965, Chap. 11.

[2]Thomson, W. T., *Introduction to Space Dynamics*, Wiley, New York, 1961, Chap. 5.

[3]Greenwood, D. T., *Principles of Dynamics*, Prentice–Hall, Englewood Cliffs, NJ, 1965, Chap. 8.

[4]Meirovitch, L., *Methods of Analytical Dynamics*, McGraw–Hill, New York, 1970, Chap. 4.

[5]Kaplan, M. H., *Modern Spacecraft Dynamics and Control*, Wiley, New York, 1976, Chap. 2.

[6]Hughes, P. C., *Spacecraft Attitude Dynamics*, Wiley, New York, 1986, Chap. 4.

[7]Kraige, L. G., and Junkins, J. L., "Perturbation Formulation for Satellite Attitude Dynamics," *Celestial Mechanics*, Vol. 13, No. 1, 1976, pp. 39–64.

[8]Kraige, L. G., and Skaar, S. B., "A Variation of Parameters Approach to the Arbitrarily Torqued, Asymmetric Rigid Body Problem," *Journal of the Astronautical Sciences*, Vol. 25, No. 3, 1977, pp. 207–226.

[9]Cochran, J. E., Jr., Shu, P. H. I., and Rew, S. D., "Attitude Motion of Asymmetric Dual-Spin Spacecraft," *Journal of Guidance, Control, and Dynamics*, Vol. 5, No. 1, 1982, pp. 37–42.

[10]Larson, V., and Likins, P. W., "Closed-Form Solution for the State Equations for Dual-Spin and Spinning Spacecraft," *Journal of the Astronautical Sciences*, Vol. 21, Nos. 5, 6, 1982, pp. 244–251.

[11]Longuski, J. M., "Real Solution for the Attitude Motion of a Self-Exited Rigid Body," *Acta Astronautica*, Vol. 25, No. 3, 1991, pp. 131–139.

[12]Tsiotras, P., and Longuski, J. M., "A Complex Analytic Solution for the Attitude Motion of a Near-Symmetric Rigid Body Under Body Fixed Torques," *Celestial Mechanics and Dynamical Astronomy*, Vol. 51, No. 3, 1991, pp. 281–301.

[13]Tsiotras, P., and Longuski, J. M., "Analytic Solutions for a Spinning Rigid Body Subject to Time-Varying Body-Fixed Torques, Part II: Time Varying Axial Torque," *Journal of Applied Mechanics*, Vol. 60, No. 3, 1993, pp. 976–981.

[14]Longuski, J. M., and Tsiotras, P., "Analytic Solutions for a Spinning Rigid Body Subject to Time-Varying Body-Fixed Torques, Part I: Constant Axial Torque," *Journal of Applied Mechanics*, Vol. 60, No. 3, 1993, pp. 970–975.